Published in final edited form as:

J Immunol. 2017 August 15; 199(4): 1453–1464. doi:10.4049/jimmunol.1700165.

Lung epithelial cell-derived microvesicles regulate macrophage migration *via* microRNA-17/221-induced integrin beta1 recycling

Heedoo Lee[1], **Duo Zhang**[1], **Jingxuan Wu**[1], **Leo E. Otterbein**[2], and **Yang Jin**[1,*]

[1]Division of Pulmonary and Critical Care Medicine, Department of Medicine, Boston University, Boston, MA 02118, USA

[2]Department of Surgery, Harvard Medical School, Beth Israel Deaconess Medical Center, Boston, MA 02215

Abstract

Robust lung inflammation is one of the prominent features in the pathogenesis of acute lung injury (ALI). Macrophage migration and recruitment are often seen at the early stage of lung inflammatory responses in response to noxious stimuli. Using an acid-inhalation induced lung injury model, we explored the mechanisms by which acid exposure initiates macrophage recruitment and migration during development of ALI. The lung epithelium comprises a large surface area and functions as a first-line defense against noxious insults. We found that acid exposure induced a remarkable microvesicle (MV) release from lung epithelium as detected in bronchoalveolar lavage fluid (BALF). Significantly elevated RNA, rather than protein, was found in these epithelium-derived MVs after acid and included several highly elevated microRNAs (miRNAs) including miR-17 and miR-221. Acid-induced-epithelial MV release promoted macrophage migration *in vitro* and recruitment into the lung *in vivo* and required, in part, MV-shuttling of miR-17 and/or miR-221. Mechanistically, acid-induced epithelial MV-miR-17/221 promoted β1 integrin recycling and presentation back onto the surface of macrophages, in part via a Rab11-mediated pathway. Integrin β1 is known to play an essential role in regulating macrophage migration. Taken together, acid-induced ALI results in epithelial MV-shuttling of miR-17/221 that in turn modulates macrophage β1 integrin recycling promoting macrophage recruitment and ultimately contribute to lung inflammation.

Keywords

microvesicle (MV); microRNA; macrophage; epithelial cell; integrin

Background

Emerging evidence has shown that extracellular vesicles (EVs) regulate diverse cellular and biological processes related to human disease by facilitating cell-cell cross-talk (1). EVs are classified into three major classes that include exosomes (Exos), microvesicles (MVs) and

*To whom correspondence should be addressed. Tel: +1-617-414-3298; Fax: +1-617-536-8093; yjin1@bu.edu.

Disclosure

The authors declare no competing financial interests

apoptotic bodies (ABs) that is based on their size and mode of generation (2, 3). The smallest EVs (Exos) have range in size from 50 to 150 nm and are generated *via* an endocytic MVB pathway (3). MVs (200 nm – 1,000 nm) and ABs (1,000 – 5,000 nm) are produced through direct budding of the plasma membrane or cellular rupture (4–6). Whereas the release of MVs is continuous, and stimulated by a variety of cell stressor, ABs are only generated as a result of cell death. In contrast MVs and Exos are continuously released by live cells (7, 8) in either the absence or presence of noxious stimuli (9, 10). Recent studies have shown that both proteins and nucleic acids are differentially sorted into the three types of EVs reflecting their functional diversity (3, 9). Accumulating evidence further suggest that in addition to EV surface antigens, EV can shuttle microRNAs (miRNAs) that may play an essential role in mediating intercellular communication (11–13). It is now generally accepted that single miRNAs have diverse targets and can up- or down-regulate hundreds of genes (14), MVs and Exos therefore act in part as messengers in the coordination of innate immune responses to noxious stimuli (7, 9, 10).

ALI/ARDS is a complex syndrome with three overlapping phases characterized by the reduction of pulmonary compliance, recruitment of inflammatory cells into the alveoli and endothelial and epithelial damage (15, 16). Due to the complexity of the pathogenesis of ARDS, developing specific and effective therapies has been exceedingly difficult. Common features of ALI/ARDS include an intense inflammatory response in the lung parenchyma, severe injury to the epithelial and endothelial cell barriers leading to alveolar edema, decreased lung compliance, impaired gas exchange and hypoxemia (17, 18). This can occur in the presence of a broad range of agents including oxidative stress, acid aspiration and infection (7, 10). The alveolar epithelium functions as a first-line defense against noxious insults and as such is critical in maintaining the integrity and function of the lung during development of ALI (17–20). In addition to functioning as a barrier, recent evidence suggests that Alveolar Type I (ATI) epithelial cells serve important functions in innate immune responses and are underappreciated in lung cell-cell communication (21). An improved understanding of the mechanisms and significance of epithelium-immune cell crosstalk in response to noxious stimuli may provide insight for new diagnostic/therapeutic approaches for treating ALI/ARDS.

Macrophages are the first responders among all immunoregulatory cells and are therefore involved in the initiation and development of lung inflammation (22–24). Macrophages present at barrier sites like the lung are surveillance cells (25, 26). How macrophages migrate and are recruited from the peripheral circulation into the lung in response to a noxious stumuli remains largely unclear and is a complex process involving diverse cellular regulatory mechanisms (27–30),

Integrins are a family of heterodimeric adhesion receptors comprised of approximately 17 α chains and eight β chains integrins that pair together in a specific pattern based on the cells in which they are expressed (31). These heterodimeric integrins have been classified into subfamilies according to the β chain that they share (31). Among the integrin subfamilies, integrin β1 and β2 serve critical roles in monocyte/macrophage extravasation and migration into sites of inflammation (27). Expression of the β2 subfamily is limited to white blood cells and is comprised of one of four heterodimeric isotypes depending on how they

combine with the α chains to form Leukocyte Function Antigen (LFA)-1, Mac-1, gp150/95 and ad/b2 (32). The β2 integrins serve as principal receptors that are recognized by complementary adhesion molecules on endothelium known as intercellular cell-adhesion molecule (ICAM)-1 and ICAM-2. The ICAM molecules are responsible for allowing leukocytes to bind to endothelial cells at sites of inflammation (27, 33). Once the leukocytes have extravasated from the circulation these differentiated monocytes/macrophages then interact with extracellular matrix (ECM) proteins through the integrin β1 subfamily (27). Integrin β1 combines with at least nine α integrins while the integrin β1 subfamily recognizes ECM proteins including fibronectin, collagen, and laminins (34). It is now generally accepted that integrin β1 is continuously internalized and traffics to Rab11-positive recycling endosomes or lysosomes to control cell migration (35, 36). Recent reports show that incorporation of integrin β1 into recycling endosomes is essential for macrophage migration (28).

Collectively, our studies sought to explore the role of epithelial MV-shuttling miRNAs in the development of lung inflammatory responses after acid-inhalation. We further describe the effects of MV-shuttling miRNAs on macrophage migration and its underlying mechanism of action involvin integrin β1 recycling.

Materials and Methods

Materials

MiRNA-17 mimics (HMI0264), miRNA-221 mimics (HMI0398), miRNA-320a mimics (HMI0470), miRNA-92a mimics (HMI0955), and HRP-conjugated anti-β-actin antibody (A3854) were purchased from Sigma Aldrich (St. Louis, MO). Mouse anti-integrin β1 (sc-374430), mouse anti PTEN (sc-7974), mouse anti-c-fos (sc-166904) and rabbit anti-flotillin-1 (sc-25506) antibodies were purchased from Santa Cruz Biotechnology (Santa Cruz, CA). Rabbit anti-Rab11 (ab128913), rabbit anti-TSG101 (ab30871), and PE-conjugated anti-pan cytokeratin antibodies were purchased from Abcam Inc. (Cambridge, MA). Rabbit anti-caveolin-1 and anti-Histone H3 antibodies were purchased from Thermo Fisher (Waltham, MA) and Cell Signaling (Danvers, MA), respectively. FITC-conjugated anti-CD11b (11-0112-82) and APC/Cy7-conjugated anti-CD11c (117323) antibodies were purchased from eBioscience (San Diego, CA) and Biolegend (San Diego, CA), respectively.

Acid-induced acute lung injury

Wild type C57BL/6 mice (6 to 8 weeks of age) were obtained from Jackson Laboratory (Bar Harbor, ME). Hydrochloric acid (0.1 N, pH 1.5) was intratracheally instilled into the mouse lung. One day after instillation, mice were sacrificed and bronchoalveolar lavage fluid (BALF) was collected, and lung tissue was harvested. All protocols and methods involving animals were approved by the Institutional Animal Care and Use Committee (IACUC) in accordance with approved guidelines.

Categorize the EVs from BALF

Previously reported protocols and techniques were applied to isolate three subpopulations of EVs from mouse BALF, including apoptotic bodies (ABs), microvesicles (MVs) and

exosomes (Exos) (9, 37, 38). BALF was centrifuged at 300 g for 5 min to remove the inflammatory cells. The supernatant was then collected and centrifuged at 2000 g for 10 min to pellet ABs (37, 38). To isolate MVs, the AB-depleted supernatant was then centrifuged at 16,000 g for 40 min (4–6). Finally, the resulting supernatant was ultracentrifuged at 100,000 g for 1 h to pellet Exos (39, 40). Each vesicles were re-suspended in cold PBS and stored at −80°C. Protein concentration was measured using a Bradford assay. Size and specific-protein makers of the three types of EVs were analyzed using dynamic light scattering (DLS) instrumentation (Brookhaven 90plus Nano-particle Sizer, Biomedical Engineering core, Boston University), and western blotting, respectively.

Bronchoalveolar lavage and inflammatory cell counts

To obtain BALF cells from mice, a bronchoalveolar lavage (BAL) was performed twice with 1 ml cold PBS. Total inflammatory cell counts in the BALF were determined using a hemocytometer as previously described (25). For cytospin preparations, cell suspension was cytocentrifuged at 300 × g for 5 min using a Shandon Cytospin 4 (Thermo Scientific, Rockford, IL). Slides were air-dried, and stained with Hema 3™ Fixative and Solutions (PROTOCOL™). Differential cell counts were evaluated under a light microscope.

Macrophage culture

Mouse bone marrow-derived macrophages (BMDMs) were isolated from mice as described previously (9). Isolated bone marrow cells were cultured with 30% L929-conditioned medium for 5 to 7 days to allow differentiation of the bone marrow monocyte / macrophage progenitors, and further experimentation. Human THP1 monocytes were obtained from the American Type Culture Collection (ATCC) and maintained in RPMI-1640 with 10% fetal bovine serum (FBS) and 1% penicillin / streptomycin. Cells were cultured at 37°C in a humidified atmosphere with 5% CO_2 and 95% air. THP1 monocytes were differentiated into macrophages with 20 ng/ml phorbol 12-myristate 13-acetate (Sigma-Aldrich) for 24 h and then further matured in fresh medium for an additional 24 h before use.

Lung epithelial cell isolation

Primary alveolar epithelial cells were isolated from mice as described previously (41). Briefly, mouse lung tissue was washed with sterile PBS, followed by infusion of 2 ml dispase and 0.5 ml 1% agarose. Lung tissue was then dissociated in DMEM with 25 mM HEPES and 200 U/ml DNase. Isolated cells were sequentially strained using 100μm, 40μm and 20μm cell strainers, followed by incubation on plates pre-coated with CD45 and CD16/32 antibodies for 2 h. Suspended cells were further transferred to non-coated plates to remove fibroblasts. After another 2 h incubation, suspended epithelial cells were cultured in DMEM containing 10% FBS prior to further experimentation.

Flow cytometry

Flow cytometric analysis of BALF-MVs was performed as described previously (40) with minor modifications. Isolated MVs were coupled to 10 μl of aldehyde/sulfate latex beads (Thermo Scientific) for 2 h, and the MV-coated beads were then treated with 4% BSA for 1 h as a blocking agent. The bead-bound MVs were then permeabilized and fixed for 5 min

with 0.2% Triton X-100 and 2% formaldehyde, followed by incubation with designated antibodies.

For analysis of BALF macrophages, cells were incubated with antibody specific to integrin β1, followed by incubation with CD11b-FITC and a PE-conjugated secondary antibody. Macrophages present in BALF was gated based on light scattering profiles, as described previously (42). FITC- and PE-conjugated secondary antibodies were used as negative controls. Flow cytometric analysis was performed using FACSCalibur instrument (BD Biosciences), and the data were analyzed using FlowJo software (Treestar, Inc.).

RNA preparation, reverse transcription, and quantitative real-time PCR

Total RNAs were purified from the isolated BALF-EVs or harvested macrophages using MiRNeasy Mini Kits (Qiagen). Purified RNA concentration was measured using the NanoDrop Lite Spectrophotometer (Thermo Scientific). A Reverse Transcription Kit (Thermo Fisher Scientific) was used to generate single stranded cDNA from equal amounts of purified RNAs. SYBR green-based real-time quantitative PCR (qPCR) was performed for measuring miRNAs as previously described (43, 44). For relative expression levels of mRNAs, beta tubulin was used as a reference housekeeping gene. The list of primers is shown in Table 1.

Direct miRNA transfection into MVs

10 pM of miRNA mimics or inhibitors were directly transfected into isolated BALF-MVs with 0.1M $CaCl_2$, as previously described (45). The transfected MVs were washed with cold PBS followed by 16,000 × g centrifugation. To confirm successful transfection, the transfected MVs were treated with RNase, which rapidly degrades miRNAs outside of MVs (46, 47). MV-containing miRNA levels were measured using qPCR (supplementary fig 1A). The transfected MVs were used for further experiments.

Vesicle uptake assay

Vesicle uptake determination was performed as previously described (48)with a minor modification. Isolated MVs were labeled with carboxyfluorescein succinimidyl ester (CSFE), followed by washing with cold PBS. WT mice (intratracheal instillation) or BMDMs were then treated with the prepared MVs for 24 h, followed by collection of BALF cells or BMDMs. The collected cells were trypsinized and washed with acid buffer (pH 2.6) to remove surface-bounded MVs (48), followed by cytospin preparation. Uptake of the MVs and the MV-containing miRNAs were analyzed using confocal microscopy and qPCR, respectively.

Integrin internalization, endocytic recycling, and degradation assay

Integrin trafficking assays were performed as previously described (49) with a minor modification. For the internalization assay, macrophage-surface proteins were biotinylated with 0.5 mg/mL Sulfo-NHS-SS Biotin (Thermo Fisher Scientific) for 20 min at 4 °C, followed by washing with TBS. Internalization of surface proteins was induced by incubating cells at 37 °C. After internalization of the surface proteins, the remaining biotin on the cell surface was stripped with 50 mM MesNa (Sigma-Aldrich), followed by

quenching of the residual MesNa with 20 mM iodoacetamide (Sigma-Aldrich). The cells were then harvested with lysis buffer containing 1% Triton X-100 and protease inhibitors. Biotinylated proteins were precipitated with streptavidin agarose (Thermo Scientific), and subjected to western blot analysis using an antibody specific to integrin β1. The percent internalization was determined using the band intensity of internalized integrin β1 relative to total labeled integrin β1 (without MesNa).

For the recycling assay, biotin-labeled, surface integrins were incubated for 30 min to allow internalization and the remaining biotin on the cell surface was stripped as described above. The internalized integrins are able to recycle back to the cell surface by incubating at 37 °C. The cell surface was then stripped again to remove the recycled integrins. Biotinylated proteins were precipitated and analyzed by Western blot analysis. The percentage of recycled integrins was determined by comparing the band intensity of the remaining integrin β1 in the cells to the total internalized integrin β1.

Degradation of cell surface integrins was performed as previously described with a minor modification (40). Surface-biotinylated macrophages were further cultured for the designated time points. Biotinylated proteins were then precipitated and the remaining integrin β1 was analyzed by Western blot analysis. The percentage of degraded integrins was calculated using the signal intensity of the remaining integrin β1 in the cells at the indicated time points relative to total labeled integrin β1.

Antibody-based integrin trafficking assay

Antibody-based trafficking assays were performed as previously described (40) with minor modifications. The surface integrins on cultured macrophages were labeled with anti-integrin β1 antibody (E-11) for 20 min at 4 °C, followed by internalization of the labeled integrin with incubation at 37 °C for 30 min. The remaining labeled integrins on the cell surface were then stripped with acid buffer (pH 2.5). The cells were then fixed and permeabilized with 100 % cold methanol for 10 min at 4 °C. Recycling endosomes were stained with anti-Rab11 IgG. The internalized integrin β1 and Rab11-postive recycling endosomes were visualized using FITC-conjugated and Alexa 594-conjugated secondary antibody, respectively, using a Leica SP5 point-scan confocal microscope (Leica Microsystem). Staining intensities and coefficient values were analyzed using ImageJ 1.51h software (NIH, Bethesda, MD).

Transwell migration assay

Macrophage migration analyses were performed using 6.5-mm-diameter polycarbonate with 8.0-μm microporous membranes (Costar, Cambridge, MA), as described previously (9). 3×10^4 macrophages were placed in the inner chamber coated with BD Matrigel™ Basement Membrane Matrix (BD bioscience). EV-depleted 10% FBS was added in the outer well with isolated BALF-MVs transfected with miRNA mimics or inhibitors. After 24 h incubation, migrated cells were fixed with 4 % formaldehyde and stained with hematoxylin. Migrated cells were counted using a light microscope.

Western Blot Analysis

Harvested cells were lysed with RIPA buffer containing 1% triton X-100, protease inhibitor, and phosphatase inhibitor. Western blotting analysis was performed as described previously (39). Densitometric analyses were performed using ImageJ software (NIH, Bethesda, MD), and the gene expression was normalized to β-actin.

ELISA

Mouse BALF was collected 24 h after acid aspiration and centrifuged at 300 g for 5 min to pellet the inflammatory cells. TNF, IL1β, IL6, IL10, and IL23 levels were analyzed using DuoSet® ELISA Development Systems (R&D system), according to the manufacturer's recommendation.

Statistical analysis

For all experiments, the exact n values and statistical significances were shown in the corresponding figure and figure legends. Represented data of the identical results were shown in the presented figures. Statistical analysis was performed with unpaired two-tailed Student's T-test. Values of $p < 0.05$ were considered statistically significant (* $p < 0.05$, ** $p < 0.01$).

Results

Lung epithelial cell-derived MVs are robustly upregulated in BALF after acid inhalation

EVs, are classified into ABs, MVs and Exos based on their size, protein markers and modes of generation. As shown figure 1A, the size of MVs (172.8 +/− 3.2 nm) measured by both DLS and NanoSight were significantly larger than Exos (122.6 +/− 1.7 nm). We also verified expression of selective protein makers for each type of EVs (fig 1B) and found that MVs were the principle form of EVs in mouse BALF after acid inhalation. 65% of EVs fell into the size range of MVs (fig 1C). More interestingly, MVs showed the greatest induction compared to other types of EVs (fig 1D). To determine the source of origin of the BALF MVs, we analyzed surface markers using antibodies against CD11b, CD11c (myeloid lineage markers) and pan cytokeratin (epithelial cell marker). As shown in figure 1E, more than 70% of BALF MVs were derived from lung epithelial cells while a small amount MVs originated from myeloid cells. Furthermore, epithelial cell-derived MVs were dramatically upregulated compared to myeloid cell-derived MVs, which showed no change or a very slight induction following acid inhalation (fig 1E).

MV-RNA is upregulated more robustly versus MV-protein in the presence of a noxious stimuli

We analyzed the composition of isolated MVs and isolated Exos. In the presence of acid exposure, both MV-RNA and MV-protein expression were enhanced. Interestingly, after normalization with MV-protein, MV-RNA remained highly elevated (fig 2A). In contrast, both Exo-RNAs and Exo-proteins while elevated after acid exposure, showed no significant up-regulation when normalizated with MV-protein (fig 2B). We next analyzed several microRNAs in the BALF of acid-induced MVs and Exos generation. MiR-221, 320a, 92a,

and 17 were significantly higher (more than 2-fold) in MVs after acid exposure. No significant alteration of these miRNAs was observed in BALF Exos (fig 2C and D).

Acid-induced lung injury promotes macrophage recruitment and lung inflammation

Macrophage activation, recruitment, and migration play an essential role in initiation of lung immune responses (9, 50–52). Acid instillation induced a massive increase in cell infiltration in both lung tissue and BALF respectively (fig 3A). Among all infiltrated cells, macrophages were the most predominant cell type present in BALF up to 24 h after acid inhalation (fig 3B). Neutrophils influx in the airways peaked 12h after acid inhalation (fig 3B) while eosinophils and lymphocytes, were detected in low amounts in the BALF (data not shown) indicating a differential cellular response in the setting of acid exposure. We also confirmed that pro-inflammatory cytokines including TNF, IL-1β, and IL-6 were significantly increased 24 h after acid inhalation in the BALF compared to sham controls (fig 3C).

Macrophages respond to epithelial cell-derived MVs and MV-miRNAs

To determine the target and recipient cells of the epithelial-derived MV-shuttling miRNAs in the BALF, we first examined expression of miR-17, 320a, 92a and 221 in the isolated lung epithelial cells and BALF inflammatory cells (70–90 % of the BALF inflammatory cells are macrophages; fig 3B). We found that levels of these mature miRNAs (mature miR-17, 320a, 92a and 221), but not their precursor forms, were dramatically decreased in the lung epithelial cells in response to acid-exposure (fig 4A). In contrast, the levels of mature miR-17/221 were highly elevated in BALF macrophages (fig 4B). In the absence of any changes in pre-miRNA expression, the increased mature forms of miR-17/221 in macrophages suggest that these mature miRNAs are, in part transferred from other cells, such as lung epithelial cells.

To directly examine MV uptake by macrophages *in vivo*, we labeled MVs with CFSE. The labeled MVs were delivered intratracheally to WT mice and BALF was collected 24h later (fig 4C). Greater than 90% of cells in the BALF were macrophages. As shown in figure 4D, we successfully visualized efficient uptake of labeled MVs by BALF macrophages. Importantly, we confirmed that uptake of acid-induced MVs led to a significant increase in miR-17 and 221, but not their precursor forms, in recipient BALF macrophages (fig 4E). This observation indicated that MVs and MV-containing miRNAs were actively delivered to macrophages *in vivo*. We also noted that miR-17 and 221 significantly upregulated expression of integrin β1, an essential complex required for macrophage recruitment and migration (27, 32, 53) (fig 4F).

Acid-induced MV-miRNAs modulate macrophage recruitment and migration in the lung

To determine the effects of MVs and MV-miRNAs on lung inflammatory responses and macrophage recruitment, we employed “loss of function” and “gain of function” approaches. Figure 5A illustrates our experimental design. We first isolated MVs from control mice or acid-treated mice. We then manipulated the miRNA compositions in these isolated MVs using miRNA mimics or inhibitors. We inserted miR-17 and 221 mimics into the MVs obtained from naive mice to augment their expression. The successful transfection of the miRNAs was confirmed using RNase (supplemental fig 1A). In separate experiments, we

inserted miR-17 and 221 inhibitors into MVs harvested from acid-exposed mice, given that these miRNAs were already up-regulated in response to acid. These modified MVs were delivered to WT mice *via* inhalation. After 24 h, BALF was harvested from the modified MV-treated mice and we observed significantly elevated BALF cell counts after inhalation of MVs enriched with miR-17/221 mimics. Treating WT mice with MVs obtained from acid exposed mice resulted in significantly elevated BALF cell counts. Interestingly, after enrichment with miR-17/221 inhibitors, the MVs obtained from acid-exposed mice failed to increase cell infiltration into the lung as measured in BALF (fig 5B). Moreover, the predominant inflammatory cells remained macrophages after MV-mediated cell recruitment, indicating that macrophages are the most likely target responding to MV (fig 5B).

Acid-induced MVs upregulate expression of integrin β1 in macrophages

As described above, integrin β1 is crucial for macrophage migration into injured sites though specific interaction with ECM (27, 32, 53). We showed that miR-17 and 221 significantly upregulated integrin β1 in macrophages (fig 4F). We confirmed that BALF macrophages expressed significantly more integrin β1 after exposure to acid (fig 6A). We next studied the effects of MVs on integrin β1 expression in macrophages *in vitro*. After confirming the efficient uptake of MVs by cultured macrophages *in vitro* (fig 6B), we treated human macrophages with PBS (Con), MVs obtained from control mice, MVs obtained from acid-treated mice, Exos obtained from control mice or Exos obtained from acid-treated mice. MVs obtained from acid-exposed mice stimulated remarkable expression of integrin β1 compared to all other treatment groups (fig 6C). Similar results were observed using mouse macrophages (fig 6D).

MV-shuttling miR-17/221 up-regulated integrin β1 in macrophages

We next evaluated the role of miR-17/221 in MV-induced up-regulation of integrin β1 expression in macrophages *in vivo* and *in vitro*. To test this, isolated MVs were delivered to WT mice *via* inhalation and BALF cells were isolated and analyzed by flow cytometry 24h later. Over-expression of miR-17/221 induced expression of integrin β1 while miR-17/221 inhibitors abolished the effects of acid-induced MVs on integrin β1 expression in macrophages (fig 7A). This observation was further confirmed with BMDMs *in vitro* by Western blot (fig 7B and supplementary fig 1A–C) and real-time PCR (fig 7C). We observed that Rab11, a Rab GTPase that associates with recycling of endocytosed proteins, was also upregulated in macrophages in a similar manner to integrin β1 (fig 7B–C). Importantly, MV-shuttling miR-17/221 had no effect on Rab4, an important regulator of vesicular transport (fig 7C).

MV-containing miR-17 and 221 induce trafficking of integrin β1 into recycling endosomes

Surface expressed integrin β1 is continuously internalized *via* endocytosis and the internalized integrins are then trafficked to Rab11-positive recycling endosomes or lysosomes (35, 36). Given that MV-shuttling miR-17/221 significantly up-regulated Rab11 (fig 7B), we next examined the effect of MV-shuttling miR-17/221 on integrin trafficking in macrophages. THP1 macrophages were transfected with miR-17/221 mimics, and upregulation of integrin β1 and Rab11 was verified (fig 4F). To assess internalization of, integrin β1 cell surface proteins were labeled with Sulfo-NHS-SS-Biotin at 4°C. The

remaining labeled proteins on the cell surface were then stripped using 50 mM MesNa, and the internalized proteins were precipitated and analyzed by Western blot. For the recycling assays, the internalized protein was recycled back to the cell surface after another 37°C incubation. The recycled proteins were then stripped again and the labeled proteins that remained in the endosomes were precipitated and analyzed by Western. Whereas the internalization of surface integrin β1 was not significantly changed (fig 8A), the cell surface representation of intracellular integrin β1 was markedly increased after overexpression of miR-17/221 mimics in THP1 macrophages (fig 8B). Moreover, the degradation of the surface integrin β1 was significantly delayed in the presence of miR-17/221 overexpression (fig 8C). Collectively, the surface integrin β1 was highly augmented secondarily to enhanced recycling and delayed degradation. Rab11 expression in miR-17/221-overexpressing macrophages was also upregulated in addition to integrin trafficking processes (fig 8A–C).

We further evaluated the effect of MV-shuttling miR-17/221 in BMDMs and as shown in figure 9A, acid-induced MVs and MV-shuttling miR-17/221 upregulated the recycling of integrin β1 in BMDMs. Significant co-localization between Rab11 and integrin β1 in BMDMs was observed after treatment of acid-induced MVs or MV-shuttling miR-17/221(fig 9B). We next performed an antibody-based surface-labeling assay as described previously (40) targeting integrin β1. As illustrated in figure 9C, surface expression of integrin β1 was internalized after incubation at 37 °C. The labeled integrin β1 that remained on the cell surface was then stripped. As shown in figure 9C, robustly elevated co-localization was observed between integrin β1 (green) and Rab11 (red) after exposure of macrophages to acid-induced MVs and MV-shuttling miR-17/221, suggesting that internalized integrin β1 traffics to Rab11-positive recycling endosomes or lysosomes. Notably, acid-induced MVs enriched with the miR-17/221 inhibitor failed to induce co-localization of integrin β1 and Rab11 confirming the functional significance of MV-containing miR-17/221(fig 9C).

MV-containing miR-17 /221 mediates macrophage migration via integrin β1

We next examined the effects of MV-shuttling miR-17/221 on macrophage migration *in vitro*. As shown in figure 10A, we seeded BMDMs in a transwell insert coated with basement membrane matrix proteins and added the following agents into the transwell lower compartment: 1) MVs obtained from control mice plus control oligos, 2) acid induced MVs plus control miRNA oligos, 3) MVs obtained from control mice enriched with miR-17/221 mimics and 4) MVs obtained from acid-exposed mice enriched with miR-17/221 inhibitors. To determine the functional role of integrin β1 in MV-mediated macrophage migration, we pretreated BMDMs with integrin β1 siRNA (fig 10B). As expected, acid-induced MVs and MV-shuttling miR-17/221 significantly induced BMDM migration compared to control MVs. The effect of acid-induced MVs was abolished after inhibition of miR-17/221 (fig 10C). We further observed that depletion of integrin β1 decreased the number of migrated cells (fig 10C). In addition, acid-induced MVs and MV-shuttling miR-17/221 failed to induce migration of the integrin β1-deficient BMDMs, indicating that MV-shuttling miR-17/221-mediated macrophage migration was, in part integrin β1 dependent (fig 10C).

Discussions

EVs refer to a group of heterogeneous vesicles with different sizes, features, mechanisms of formation and function (1–3, 5, 40, 54, 55). Depending on the cellular sources and stimuli, EVs are generated *via* direct budding (MVs), secretion from cells *via* multivesicular bodies (MVBs, Exos) or formation by plasma membrane blebbing after undergoing apoptosis (ABs). Proteins derived from parent cells are often detectable in EVs such as surfactant proteins (SPs) that can be found in EVs released from lung epithelial cells (26). We previously reported that development of hyperoxia-induced lung injury (HALI) is influenced by BALF EVs from lung epithelium (9, 26). Here, we confirmed that epithelial cells are the likely source of BALF EVs during the development of ALI, regardless of the noxious stimuli. We put forth that lung epithelium-derived EVs are dominant participants primarily in “sterile” stimuli-induced ALI. In the setting of bacterial infection-associated ALI, such as bacterial pneumonia, a large amount of BALF EVs are derived from macrophages, other immunomodulatory cells, and bacteria themselves (unpublished data). While the pathogenesis of acid-induced lung injury is significantly different when compared to HALI, we found that MVs remained the principle type of EVs present in BALF and that MV-RNAs were robustly altered after acid exposure. This is consistent with our previous reports with HALI (9). Whether these observations remain the same in the setting of pathogen-induced lung injury requires further investigation.

Our previous reports using the HALI model suggest that epithelial MVs mediate the cross-talk between lung epithelial cells and alveolar macrophages via MV-shuttling miRNAs (9). However, a different MV-miRNA repertoire is involved in acid-induced lung injury, compared with those involved in HALI. In the current study, we demonstrated how epithelial MVs promote macrophage recruitment and migration into the lung. In the absence of infectious stimuli, the lung epithelium plays an essential role in releasing chemoattractants that target circulating macrophages. The role of alveolar epithelial cell-mediated chemokine/cytokine release has been well documented (26, 56, 57). Here, we show that epithelial MVs and MV-shuttling miRNAs modulate, in part, macrophage recruitment and migration. Unlike chemokines, MV-shuttling miRNAs directly regulate the cellular machinery necessary for macrophage migration and include cell surface expressed integrin β1 expression.

The integrin β1 chain and distinct α chains can form at least nine heterodimer combinations (27, 34) that permit a wide variety of αβ combinations while sharing a common β1 chain. These adhesion molecules interact with a diverse array of ECM proteins. We investigated the effects of MV-shuttling miR-17/221 on expression of integrin β1 in monocytes and macrophages. It has been reported that the integrin β1/Scr/PI-3 kinase-mediated signaling, but not integrin β1/focal adhesion kinase-mediated signaling, regulates macrophage migration (58, 59). Moreover, the incorporation of integrin β1-containing recycling endosomes onto their leading edge is critical for macrophage migration (28).

Collectively, our results suggest that epithelial MVs and MV-shuttling miR-17/221 up-regulate β1 integrin expression in macrophages. Further, our findings indicate that epithelial MVs and MV-shuttling miR-17/221 promote β1 integrin recycling in part through a Rab 11-mediated pathway. Rab11 belongs to the Rab family of small GTPases and regulates

membrane trafficing (36). Rab11 in particular regulates recycling of endocytosed proteins and is used as a recycling endosomal marker (36, 40). Co-localization of Rab11 and integrin β1 suggests that integrin β1 is likely recycled with recycling endosomes and regulated by Rab11.

Recent studies demonstrate that PTEN is a direct target of both miR-17 and 221 (60–62). PTEN negatively regulates macrophage infiltration (63) and suppresses expression of c-fos, a transcriptional factor involved in regulation of Rab11 (64, 65). miR-17 and 221 reduce PTEN expression and induce c-fos /Rab11 expression in macrophages (supplement figure 1D–E). These results indicate a potential molecular mechanism of action involved in miR-17/221-mediated Rab11 upregulation. Multiple miRNAs, such as miR-451, 155, and 26a have also been shown to regulate macrophage migration (66–68) and presumably other miRNAs can contribute to how macrophages respond to noxious stimuli and marginate into tissue.

There are several pitfalls in our current studies. First, it is difficult to quantify the amount or copy number of specific miRNAs generation. Therefore, it is also difficult to determine the amount of MVs that are required to deliver enough miR-17/221 oligos to trigger integrin β1 recycling and macrophage migration. Furthermore, our functional studies utililized gain and loss of function approaches using synthetic miRNA mimics or inhibitors. Due to the complexity of MV-miRNA profiles, a dose-response effect has been extremely difficult to achieve using synthetic miRNA inhibitors or mimics. Furthermore, our studies clearly show that multiple MV-miRNAs were altered after acid-inhalation. It is very likely that a MV-miRNA “signature” or “repertoire”, rather than one specific miRNA impart synergistic effects on macrophage migration and activation. Based on pulmonary anatomy, it is very possible that epithelium-derived microvesicles are successfully delivered to the monocytes and interstitial macrophages.

Given that the integrin β1 subfamily is required for interacting with ECM protein to allow leukocyte/macrophage extravasation into injured sites, (27, 32, 53) it is very likely that MV-shuttling miRNAs also regulate β2 integrins and thus, synergistically promote macrophage migration. Our future directions in acid-induced ALI include MV-miRNA profiling, quantification of each specific miRNA, dose ranging and kinetics of the MV-miRNA-regulated integrin β1 recycling and macrophage migration, and the effects of acid-induced MVs / MV-shuttling miRNA repertoires on the level of integrin β2 and α chain integrin expression.

In summary, we illustrate a novel mechanism by which lung epithelial cells directly promote macrophage migration and recruitment into the airways, in the setting of acid-inhalation-acute lung injury. Lung epithelial cell-derived MVs and MV-shuttling miRNAs imparted their effects on macrophage migration *via* enhancing β1 integrin recycling in the macrophages. Modulation of MV function and miRNA delivery may direct new avenues for therapeutic use in acute lung injury.

Supplementary Material

Refer to Web version on PubMed Central for supplementary material.

Acknowledgments

We thank Dr. Bruce Levy and his laboratory for their help on the acid-aspiration models.

This work is support by NIH R01HL102076 (Y.J.), NIH R21 AI121644 (Y.J.) and NIH R01 GM111313 (Y.J.)

References

1. Tkach M, Thery C. Communication by Extracellular Vesicles: Where We Are and Where We Need to Go. Cell. 2016; 164:1226–1232. [PubMed: 26967288]
2. Xu R, Greening DW, Zhu HJ, Takahashi N, Simpson RJ. Extracellular vesicle isolation and characterization: toward clinical application. J Clin Invest. 2016; 126:1152–1162. [PubMed: 27035807]
3. Crescitelli R, Lasser C, Szabo TG, Kittel A, Eldh M, Dianzani I, Buzas EI, Lotvall J. Distinct RNA profiles in subpopulations of extracellular vesicles: apoptotic bodies, microvesicles and exosomes. J Extracell Vesicles. 2013; 2
4. Han CZ, Juncadella IJ, Kinchen JM, Buckley MW, Klibanov AL, Dryden K, Onengut-Gumuscu S, Erdbrugger U, Turner SD, Shim YM, Tung KS, Ravichandran KS. Macrophages redirect phagocytosis by non-professional phagocytes and influence inflammation. Nature. 2016; 539:570–574. [PubMed: 27820945]
5. Clancy JW, Sedgwick A, Rosse C, Muralidharan-Chari V, Raposo G, Method M, Chavrier P, D'Souza-Schorey C. Regulated delivery of molecular cargo to invasive tumour-derived microvesicles. Nat Commun. 2015; 6:6919. [PubMed: 25897521]
6. Zhang HM, Li Q, Zhu X, Liu W, Hu H, Liu T, Cheng F, You Y, Zhong Z, Zou P, Li Q, Chen Z, Guo AY. miR-146b-5p within BCR-ABL1-Positive Microvesicles Promotes Leukemic Transformation of Hematopoietic Cells. Cancer Res. 2016; 76:2901–2911. [PubMed: 27013199]
7. Lee H, Zhang D, Minhas J, Jin Y. Extracellular Vesicles Facilitate the Intercellular Communications in the Pathogenesis of Lung Injury. Cell Dev Biol. 2016; 5
8. Thery C, Ostrowski M, Segura E. Membrane vesicles as conveyors of immune responses. Nat Rev Immunol. 2009; 9:581–593. [PubMed: 19498381]
9. Lee H, Zhang D, Zhu Z, Dela Cruz CS, Jin Y. Epithelial cell-derived microvesicles activate macrophages and promote inflammation via microvesicle-containing microRNAs. Sci Rep. 2016; 6:35250. [PubMed: 27731391]
10. Soni S, Wilson MR, O'Dea KP, Yoshida M, Katbeh U, Woods SJ, Takata M. Alveolar macrophage-derived microvesicles mediate acute lung injury. Thorax. 2016; 71:1020–1029. [PubMed: 27287089]
11. Zhang L, Zhang S, Yao J, Lowery FJ, Zhang Q, Huang WC, Li P, Li M, Wang X, Zhang C, Wang H, Ellis K, Cheerathodi M, McCarty JH, Palmieri D, Saunus J, Lakhani S, Huang S, Sahin AA, Aldape KD, Steeg PS, Yu D. Microenvironment-induced PTEN loss by exosomal microRNA primes brain metastasis outgrowth. Nature. 2015; 527:100–104. [PubMed: 26479035]
12. Fong MY, Zhou W, Liu L, Alontaga AY, Chandra M, Ashby J, Chow A, O'Connor ST, Li S, Chin AR, Somlo G, Palomares M, Li Z, Tremblay JR, Tsuyada A, Sun G, Reid MA, Wu X, Swiderski P, Ren X, Shi Y, Kong M, Zhong W, Chen Y, Wang SE. Breast-cancer-secreted miR-122 reprograms glucose metabolism in premetastatic niche to promote metastasis. Nat Cell Biol. 2015; 17:183–194. [PubMed: 25621950]
13. Ha M, Kim VN. Regulation of microRNA biogenesis. Nat Rev Mol Cell Biol. 2014; 15:509–524. [PubMed: 25027649]
14. Selbach M, Schwanhausser B, Thierfelder N, Fang Z, Khanin R, Rajewsky N. Widespread changes in protein synthesis induced by microRNAs. Nature. 2008; 455:58–63. [PubMed: 18668040]

15. Martin TR. Cytokines and the acute respiratory distress syndrome (ARDS): a question of balance. Nat Med. 1997; 3:272–273. [PubMed: 9055847]
16. Matthay MA, Ware LB, Zimmerman GA. The acute respiratory distress syndrome. J Clin Invest. 2012; 122:2731–2740. [PubMed: 22850883]
17. Whitsett JA, Alenghat T. Respiratory epithelial cells orchestrate pulmonary innate immunity. Nat Immunol. 2015; 16:27–35. [PubMed: 25521682]
18. Nold MF, Nold-Petry CA, Zepp JA, Palmer BE, Bufler P, Dinarello CA. IL-37 is a fundamental inhibitor of innate immunity. Nat Immunol. 2010; 11:1014–1022. [PubMed: 20935647]
19. Lamm WJ, Luchtel D, Albert RK. Sites of leakage in three models of acute lung injury. J Appl Physiol (1985). 1988; 64:1079–1083. [PubMed: 3366730]
20. Li X, Shu R, Filippatos G, Uhal BD. Apoptosis in lung injury and remodeling. J Appl Physiol (1985). 2004; 97:1535–1542. [PubMed: 15358756]
21. Yamamoto K, Ferrari JD, Cao Y, Ramirez MI, Jones MR, Quinton LJ, Mizgerd JP. Type I alveolar epithelial cells mount innate immune responses during pneumococcal pneumonia. J Immunol. 2012; 189:2450–2459. [PubMed: 22844121]
22. Matute-Bello G, Frevert CW, Martin TR. Animal models of acute lung injury. Am J Physiol Lung Cell Mol Physiol. 2008; 295:L379–399. [PubMed: 18621912]
23. Divangahi M, King IL, Pernet E. Alveolar macrophages and type I IFN in airway homeostasis and immunity. Trends Immunol. 2015; 36:307–314. [PubMed: 25843635]
24. Kopf M, Schneider C, Nobs SP. The development and function of lung-resident macrophages and dendritic cells. Nat Immunol. 2015; 16:36–44. [PubMed: 25521683]
25. Gauna AE, Cha S. Akt2 deficiency as a therapeutic strategy protects against acute lung injury. Immunotherapy. 2014; 6:377–380. [PubMed: 24815778]
26. Moon HG, Cao Y, Yang J, Lee JH, Choi HS, Jin Y. Lung epithelial cell-derived extracellular vesicles activate macrophage-mediated inflammatory responses via ROCK1 pathway. Cell Death Dis. 2015; 6:e2016. [PubMed: 26658190]
27. Reyes-Reyes M, Mora N, Gonzalez G, Rosales C. beta1 and beta2 integrins activate different signalling pathways in monocytes. Biochem J. 2002; 363:273–280. [PubMed: 11931654]
28. Veale KJ, Offenhauser C, Whittaker SP, Estrella RP, Murray RZ. Recycling endosome membrane incorporation into the leading edge regulates lamellipodia formation and macrophage migration. Traffic. 2010; 11:1370–1379. [PubMed: 20604897]
29. Jones GE. Cellular signaling in macrophage migration and chemotaxis. J Leukoc Biol. 2000; 68:593–602. [PubMed: 11073096]
30. Ridley AJ. Regulation of macrophage adhesion and migration by Rho GTP-binding proteins. J Microsc. 2008; 231:518–523. [PubMed: 18755007]
31. Ruoslahti E, Reed JC. Anchorage dependence, integrins, and apoptosis. Cell. 1994; 77:477–478. [PubMed: 8187171]
32. Springer TA. Adhesion receptors of the immune system. Nature. 1990; 346:425–434. [PubMed: 1974032]
33. Arnaout MA. Leukocyte adhesion molecules deficiency: its structural basis, pathophysiology and implications for modulating the inflammatory response. Immunol Rev. 1990; 114:145–180. [PubMed: 1973407]
34. Ruoslahti E. Integrins. J Clin Invest. 1991; 87:1–5. [PubMed: 1985087]
35. Pellinen T, Ivaska J. Integrin traffic. J Cell Sci. 2006; 119:3723–3731. [PubMed: 16959902]
36. Caswell PT, Norman JC. Integrin trafficking and the control of cell migration. Traffic. 2006; 7:14–21. [PubMed: 16445683]
37. Atkin-Smith GK, Paone S, Zanker DJ, Duan M, Phan TK, Chen W, Hulett MD, Poon IK. Isolation of cell type-specific apoptotic bodies by fluorescence-activated cell sorting. Sci Rep. 2017; 7:39846. [PubMed: 28057919]
38. Atkin-Smith GK, Tixeira R, Paone S, Mathivanan S, Collins C, Liem M, Goodall KJ, Ravichandran KS, Hulett MD, Poon IK. A novel mechanism of generating extracellular vesicles during apoptosis via a beads-on-a-string membrane structure. Nat Commun. 2015; 6:7439. [PubMed: 26074490]

39. Lee HD, Koo BH, Kim YH, Jeon OH, Kim DS. Exosome release of ADAM15 and the functional implications of human macrophage-derived ADAM15 exosomes. FASEB J. 2012; 26:3084–3095. [PubMed: 22505472]
40. Lee HD, Kim YH, Kim DS. Exosomes derived from human macrophages suppress endothelial cell migration by controlling integrin trafficking. Eur J Immunol. 2014; 44:1156–1169. [PubMed: 24338844]
41. Liang X, Wei SQ, Lee SJ, Fung JK, Zhang M, Tanaka A, Choi AM, Jin Y. p62 sequestosome 1/light chain 3b complex confers cytoprotection on lung epithelial cells after hyperoxia. Am J Respir Cell Mol Biol. 2013; 48:489–496. [PubMed: 23333919]
42. Shreiner AB, Murdock BJ, Sadighi Akha AA, Falkowski NR, Christensen PJ, White ES, Hogaboam CM, Huffnagle GB. Repeated exposure to Aspergillus fumigatus conidia results in CD4+ T cell-dependent and -independent pulmonary arterial remodeling in a mixed Th1/Th2/Th17 microenvironment that requires interleukin-4 (IL-4) and IL-10. Infect Immun. 2012; 80:388–397. [PubMed: 22064716]
43. Zhang D, Lee H, Cao Y, Dela Cruz CS, Jin Y. MiR-185 mediates lung epithelial cell death after oxidative stress. Am J Physiol Lung Cell Mol Physiol. 2016 ajplung 00392 02015.
44. Chen C, Ridzon DA, Broomer AJ, Zhou Z, Lee DH, Nguyen JT, Barbisin M, Xu NL, Mahuvakar VR, Andersen MR, Lao KQ, Livak KJ, Guegler KJ. Real-time quantification of microRNAs by stem-loop RT-PCR. Nucleic Acids Res. 2005; 33:e179. [PubMed: 16314309]
45. Zhang D, Lee H, Zhu Z, Minhas JK, Jin Y. Enrichment of selective miRNAs in exosomes and delivery of exosomal miRNAs in vitro and in vivo. Am J Physiol Lung Cell Mol Physiol. 2017; 312:L110–L121. [PubMed: 27881406]
46. Koga Y, Yasunaga M, Moriya Y, Akasu T, Fujita S, Yamamoto S, Matsumura Y. Exosome can prevent RNase from degrading microRNA in feces. J Gastrointest Oncol. 2011; 2:215–222. [PubMed: 22811855]
47. Cheng L, Sharples RA, Scicluna BJ, Hill AF. Exosomes provide a protective and enriched source of miRNA for biomarker profiling compared to intracellular and cell-free blood. J Extracell Vesicles. 2014; 3
48. Feng D, Zhao WL, Ye YY, Bai XC, Liu RQ, Chang LF, Zhou Q, Sui SF. Cellular internalization of exosomes occurs through phagocytosis. Traffic. 2010; 11:675–687. [PubMed: 20136776]
49. Steinberg F, Heesom KJ, Bass MD, Cullen PJ. SNX17 protects integrins from degradation by sorting between lysosomal and recycling pathways. J Cell Biol. 2012; 197:219–230. [PubMed: 22492727]
50. Fillion I, Ouellet N, Simard M, Bergeron Y, Sato S, Bergeron MG. Role of chemokines and formyl peptides in pneumococcal pneumonia-induced monocyte/macrophage recruitment. J Immunol. 2001; 166:7353–7361. [PubMed: 11390486]
51. Gonzalo JA, Lloyd CM, Wen D, Albar JP, Wells TN, Proudfoot A, Martinez AC, Dorf M, Bjerke T, Coyle AJ, Gutierrez-Ramos JC. The coordinated action of CC chemokines in the lung orchestrates allergic inflammation and airway hyperresponsiveness. J Exp Med. 1998; 188:157–167. [PubMed: 9653092]
52. Huffnagle GB, Strieter RM, Standiford TJ, McDonald RA, Burdick MD, Kunkel SL, Toews GB. The role of monocyte chemotactic protein-1 (MCP-1) in the recruitment of monocytes and CD4+ T cells during a pulmonary Cryptococcus neoformans infection. J Immunol. 1995; 155:4790–4797. [PubMed: 7594481]
53. Shang XZ, Issekutz AC. Beta 2 (CD18) and beta 1 (CD29) integrin mechanisms in migration of human polymorphonuclear leucocytes and monocytes through lung fibroblast barriers: shared and distinct mechanisms. Immunology. 1997; 92:527–535. [PubMed: 9497495]
54. Malda J, Boere J, van de Lest CH, van Weeren PR, Wauben MH. Extracellular vesicles - new tool for joint repair and regeneration. Nat Rev Rheumatol. 2016; 12:243–249. [PubMed: 26729461]
55. Budnik V, Ruiz-Canada C, Wendler F. Extracellular vesicles round off communication in the nervous system. Nat Rev Neurosci. 2016; 17:160–172. [PubMed: 26891626]
56. Jiang D, Liang J, Noble PW. Regulation of non-infectious lung injury, inflammation, and repair by the extracellular matrix glycosaminoglycan hyaluronan. Anat Rec (Hoboken). 2010; 293:982–985. [PubMed: 20186964]

57. Tao F, Kobzik L. Lung macrophage-epithelial cell interactions amplify particle-mediated cytokine release. Am J Respir Cell Mol Biol. 2002; 26:499–505. [PubMed: 11919087]
58. Meng F, Lowell CA. A beta 1 integrin signaling pathway involving Src-family kinases, Cbl and PI-3 kinase is required for macrophage spreading and migration. EMBO J. 1998; 17:4391–4403. [PubMed: 9687507]
59. Brunton VG, MacPherson IR, Frame MC. Cell adhesion receptors, tyrosine kinases and actin modulators: a complex three-way circuitry. Biochim Biophys Acta. 2004; 1692:121–144. [PubMed: 15246683]
60. Shan SW, Fang L, Shatseva T, Rutnam ZJ, Yang X, Du W, Lu WY, Xuan JW, Deng Z, Yang BB. Mature miR-17-5p and passenger miR-17-3p induce hepatocellular carcinoma by targeting PTEN, GalNT7 and vimentin in different signal pathways. J Cell Sci. 2013; 126:1517–1530. [PubMed: 23418359]
61. Li J, Yao L, Li G, Ma D, Sun C, Gao S, Zhang P, Gao F. miR-221 Promotes Epithelial-Mesenchymal Transition through Targeting PTEN and Forms a Positive Feedback Loop with beta-catenin/c-Jun Signaling Pathway in Extra-Hepatic Cholangiocarcinoma. PLoS One. 2015; 10:e0141168. [PubMed: 26501139]
62. Zhou Y, Yang Q, Xu H, Zhang J, Deng H, Gao H, Yang J, Zhao D, Liu F. miRNA-221-3p Enhances the Secretion of Interleukin-4 in Mast Cells through the Phosphatase and Tensin Homolog/p38/Nuclear Factor-kappaB Pathway. PLoS One. 2016; 11:e0148821. [PubMed: 26901347]
63. Armstrong CW, Maxwell PJ, Ong CW, Redmond KM, McCann C, Neisen J, Ward GA, Chessari G, Johnson C, Crawford NT, LaBonte MJ, Prise KM, Robson T, Salto-Tellez M, Longley DB, Waugh DJ. PTEN deficiency promotes macrophage infiltration and hypersensitivity of prostate cancer to IAP antagonist/radiation combination therapy. Oncotarget. 2016; 7:7885–7898. [PubMed: 26799286]
64. Gebhardt C, Breitenbach U, Richter KH, Furstenberger G, Mauch C, Angel P, Hess J. c-Fos-dependent induction of the small ras-related GTPase Rab11a in skin carcinogenesis. Am J Pathol. 2005; 167:243–253. [PubMed: 15972968]
65. Koul D, Shen R, Shishodia S, Takada Y, Bhat KP, Reddy SA, Aggarwal BB, Yung WK. PTEN down regulates AP-1 and targets c-fos in human glioma cells via PI3-kinase/Akt pathway. Mol Cell Biochem. 2007; 300:77–87. [PubMed: 17235455]
66. Zhang E, Wu Y. Dual effects of miR-155 on macrophages at different stages of atherosclerosis: LDL is the key? Med Hypotheses. 2014; 83:74–78. [PubMed: 24767942]
67. Chai ZT, Zhu XD, Ao JY, Wang WQ, Gao DM, Kong J, Zhang N, Zhang YY, Ye BG, Ma DN, Cai H, Sun HC. microRNA-26a suppresses recruitment of macrophages by down-regulating macrophage colony-stimulating factor expression through the PI3K/Akt pathway in hepatocellular carcinoma. J Hematol Oncol. 2015; 8:56. [PubMed: 26021873]
68. Bandres E, Bitarte N, Arias F, Agorreta J, Fortes P, Agirre X, Zarate R, Diaz-Gonzalez JA, Ramirez N, Sola JJ, Jimenez P, Rodriguez J, Garcia-Foncillas J. microRNA-451 regulates macrophage migration inhibitory factor production and proliferation of gastrointestinal cancer cells. Clin Cancer Res. 2009; 15:2281–2290. [PubMed: 19318487]
69. Paranjpe M, Muller-Goymann CC. Nanoparticle-mediated pulmonary drug delivery: a review. Int J Mol Sci. 2014; 15:5852–5873. [PubMed: 24717409]
70. Kreyling WG, Hirn S, Schleh C. Nanoparticles in the lung. Nat Biotechnol. 2010; 28:1275–1276. [PubMed: 21139613]

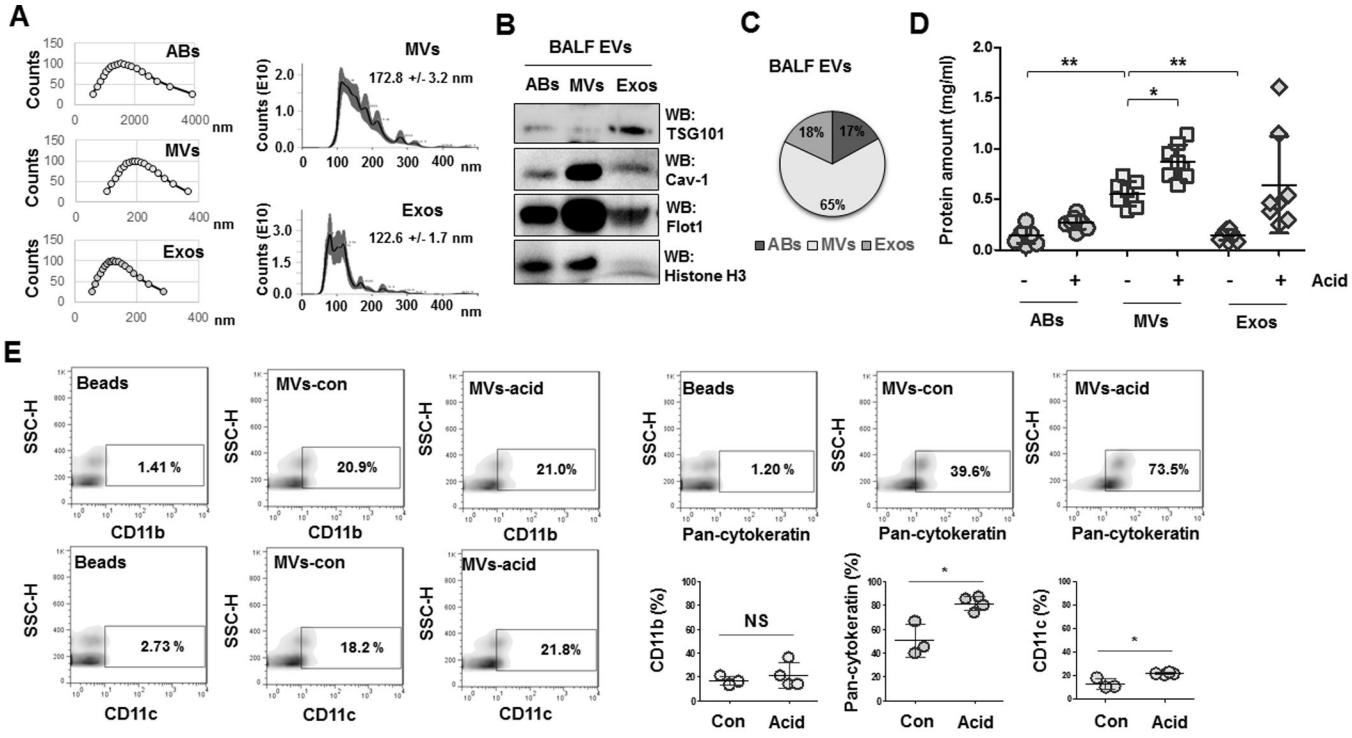

Figure 1. Characterization of the extracellular vesicles (EV) in the lung

A. Three subpopulations of EVs were isolated from mouse BALF, including apoptotic bodies (ABs), microvesicles (MVs), and exosomes (Exos). The sizes of the isolated EVs were measured using Dynamic Light Scattering (DLS) (**A**, left panel) and NanoSight (**A**, right panel). **B.** Representative Western blot of isolated EVs. **C.** Pie graph indicates the average percentages of each type of EVs isolated from BALF (n = 8 mice per group). **D.** Acid (0.1 N HCl) was intratracheally instilled into the lungs of mice. 24 h later BALF-EVs were isolated and the amount of EVs were determined. Data represent mean ± SD (n = 8 mice per group). **E.** Flow cytometry of isolated MVs to determine the proportion of cell-type-specific markers. Dot graphs show the percentages of the indicated cell markers (**E**, right lower panel). For A and B, data are representative of three independent experiments.

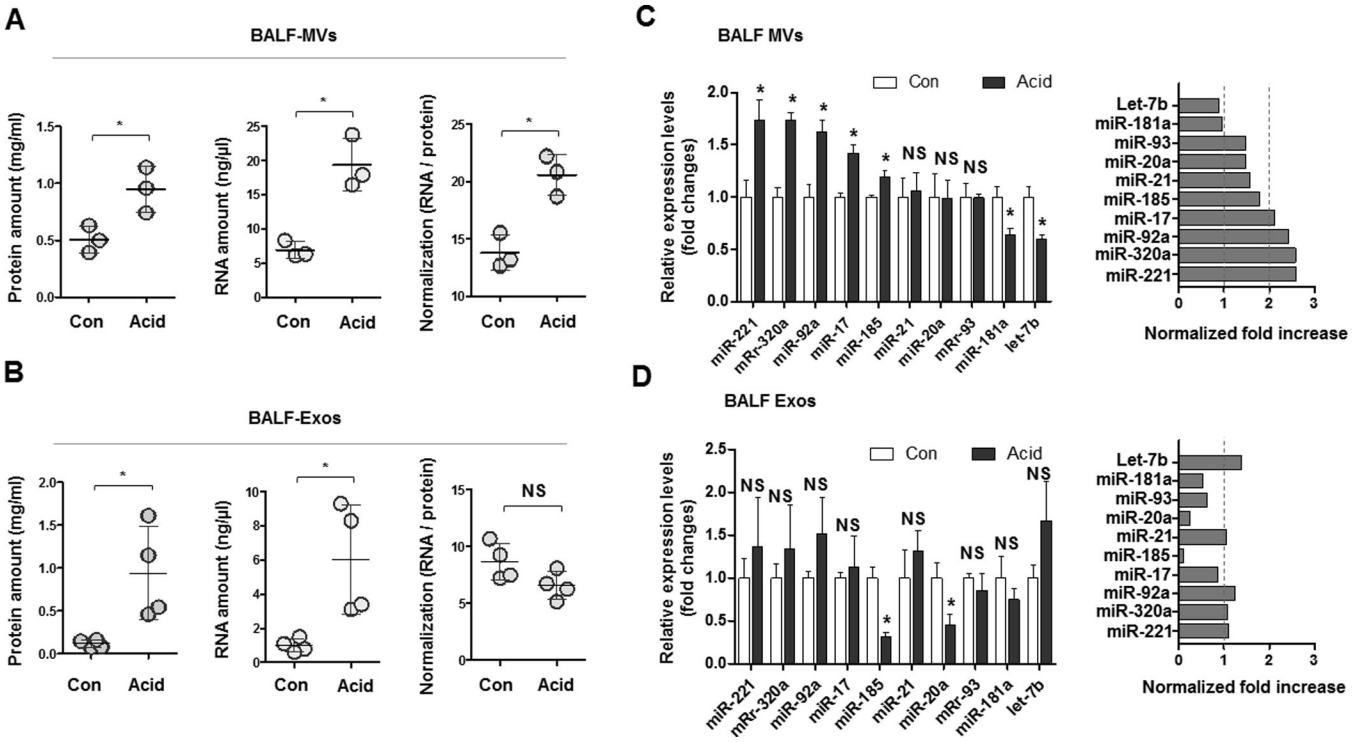

Figure 2. Expression of miRNAs in BALF-EVs after acid aspiration

(**A–B**) MVs (A) and Exos (B) were isolated from BALF after acid administration. Protein, RNA, and normalized RNA (RNA / protein) amount are shown. (**C–D**) Expression of miRNAs in MVs (**C**) and Exos (**D**) by real-time quantitative RCR (qPCR). Left panels show the fold change of miRNAs after normalization with EV-RNAs. Right panels show the fold increase in miRNAs after normalization with EV-protein.

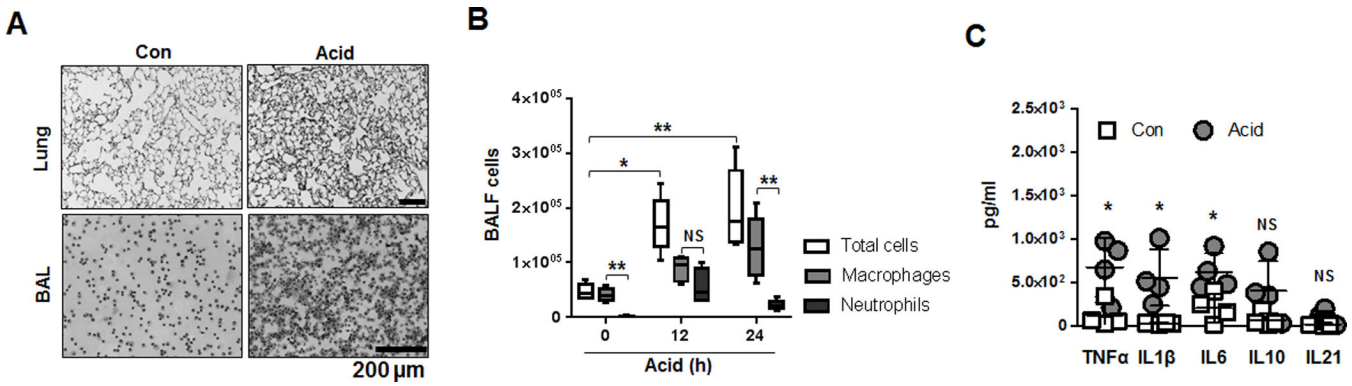

Figure 3. Acid-induced lung injury promotes macrophage recruitment and lung inflammation

A–B. H&E staining of mouse lung tissue and BALF cells 24 h after acid aspiration. Data represent mean ± SD (n = 4–6 mice per group). **C.** Cytokine expression in BALF 24 h after acid,

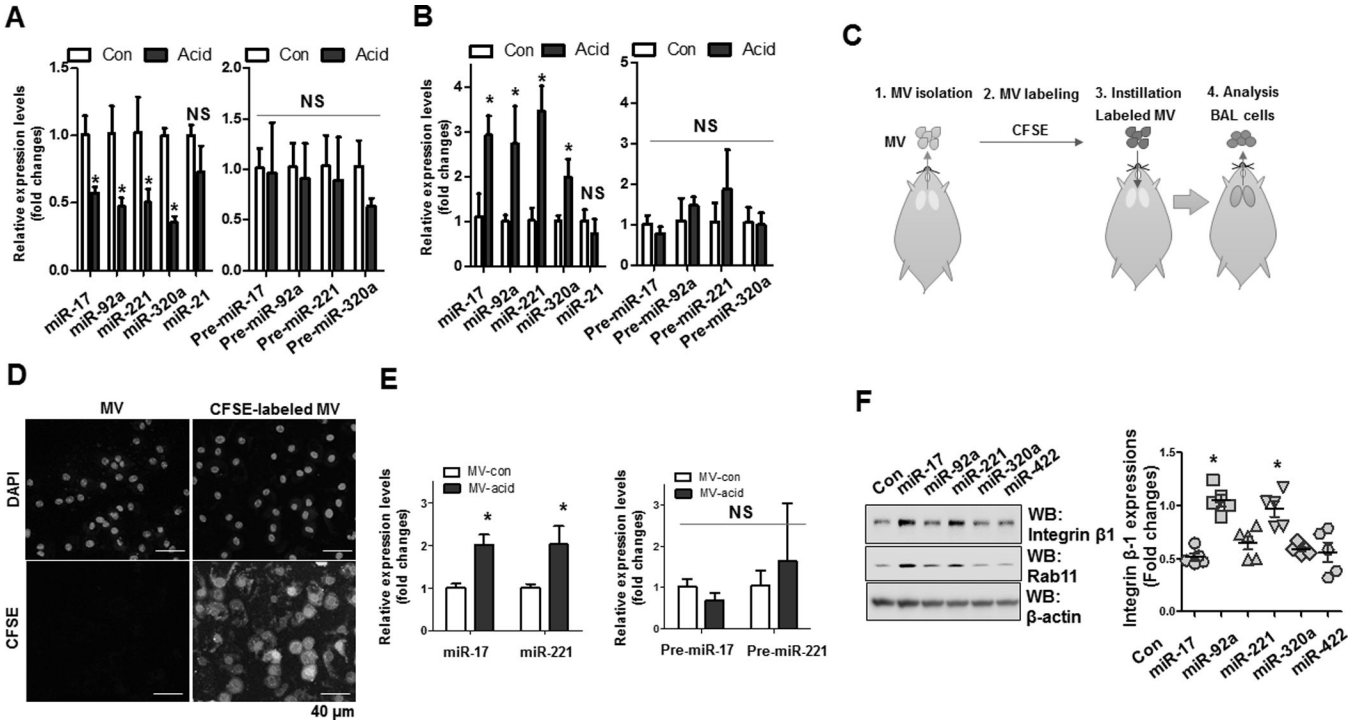

Figure 4. MVs and MV-containing miR-17/221 are actively transferred from lung epithelial cells to recipient macrophages

A–B. pPCR analysis of lung epithelial cells (**A**) and BALF cells (**B**) 24 h after acid instillation. Data represent mean ± SD (n = 4 per group). **C–D.** Schematic illustration of MV uptake analysis *in vivo* (C). CFSE-labeled MVs (D) or acid-induced MVs. **E.** MV uptake after intratracheally instillation into the lungs of mice. Data represent mean ± SD (n = 3 per group). **F.** Western blot analysis of THP1-differentiated macrophages transfected with the indicated miRNA mimics. Graph shows expression levels of integrin β1 in the transfected macrophages.

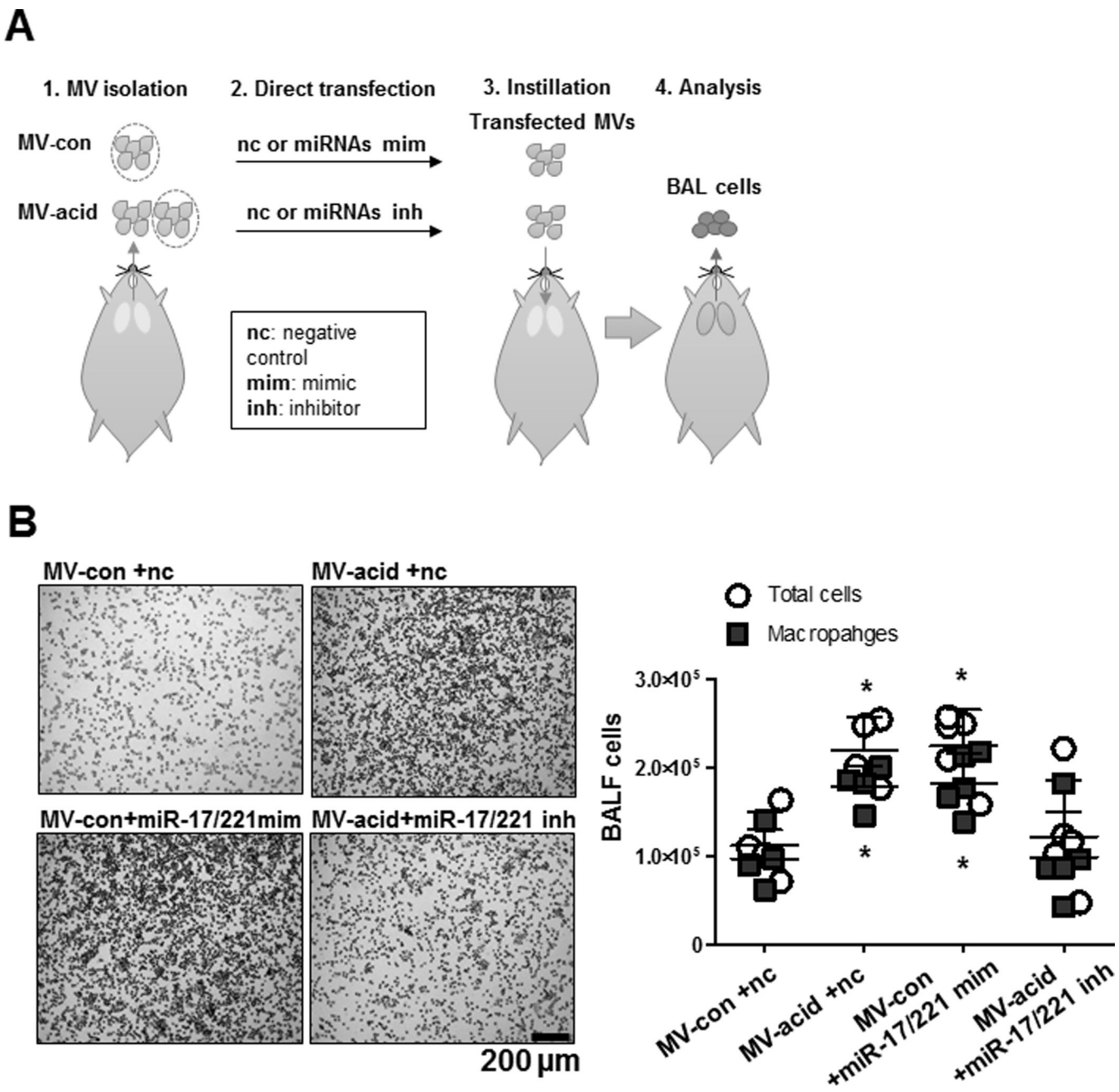

Figure 5. MV-containing miR-17/221 facilitate macrophage recruitment into the lung

A. Schematic illustration of the functional analysis of MV-containing miRNAs on macrophage recruitment *in vivo*. MVs isolated from control mice (MV-con) and mice after acid aspiration (MV-acid) and were then transfected with miR-17 and 221 mimics (MV-con +miR-17/221 mim) and inhibitors (MV-acid +miR-17/221 inh). Non-specific RNA oligos were transfected into MVs as negative controls (MV-con +nc and MV-acid +nc). 24 h after instillation, BALF cells were isolated and stained with H&E (**B**, left panel). Dot graph showed the total cell count and macrophage count in the BALF (B, right panel).

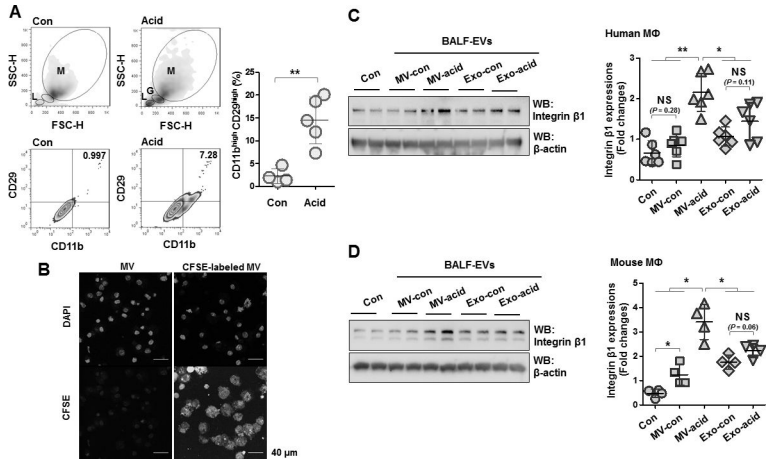

Figure 6. Acid-induced MVs up-regulate expression of integrin β1 in macrophages

A. BALF cells were isolated 24 h after acid aspiration. Based on the light-scattering profiles, BALF macrophages were gated (M: macrophages, L: lymphocytes and G: granulocytes). Expression levels of CD11b (macrophage marker) and CD29 (integrin β1) in the macrophages were measured using flow cytometry. Dot graph show the percentage of $CD11b^{high}$ $CD29^{high}$ cells. Data represent mean ± SD (n = 4 mice per group). **B.** Mouse bone marrow-derived macrophages (BMDMs) were treated with CFSE-labeled MVs for 1 day, followed by MV uptake assay, as described in Materials and Methods. **C–D.** Two types of EVs were isolated from control mice (MV-con and Exo-con) and mice after acid instillation (MV-acid and Exo-acid). **C–D.** Human THP1-differenciated macrophages and BMDMs were treated with the isolated EVs for 1day, followed by Western blot analysis. Left panel shows expression levels in treated macrophages of integrin β1 as dot graphs. Right panels show representative images of the Western blot analysis. Data represent mean ± SD (n = 4 or 6 per group).

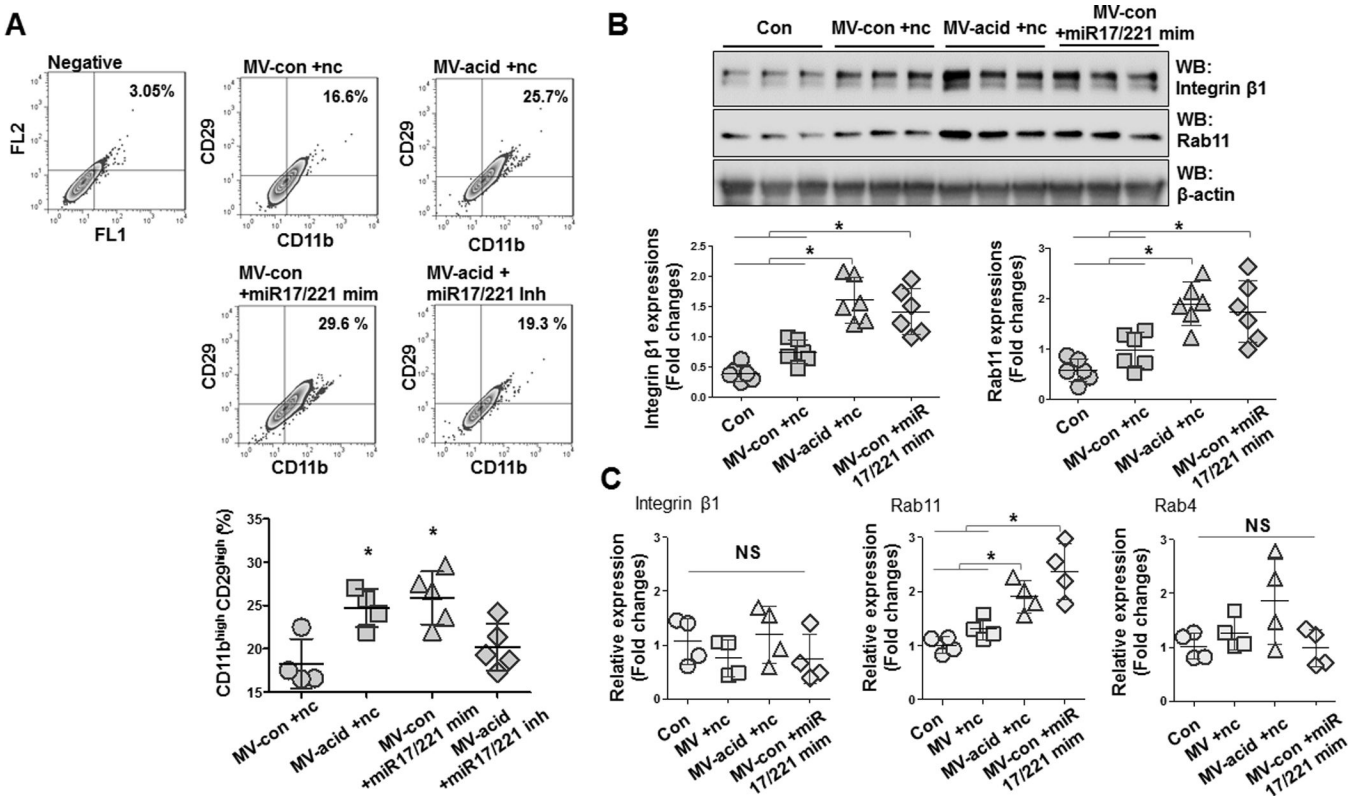

Figure 7. MV-containing miR-17/221 upregulate integrin β1 in macrophages

A. BALF-MVs were isolated from control mice (MV-con) and mice after acid instillation (MV-acid). miR-17 and 221 mimics (MV-acid +miR-17/221 mim) and inhibitors (MV-con +miR-17/221 inh) were directly transfected into MV-con and MV-acid, respectively. Non-specific RNA oligos were transfected into MVs as negative controls (MV-con +nc and MV-acid +nc). The transfected MVs (20 μg/30 μl/mouse) were intratracheally instilled into mice. 24 h after instillation, BALF cells were isolated and gated by flow cytometry for $CD11b^{high}$ $CD29^{high}$. Data represent mean ± SD (n = 4 or 5 mice per group). **B–C.** BALF-MVs were prepared as described in (A). BMDMs were treated with the MVs (5 μg/500 μl/well) for 24 h, followed by Western blot (**B**), and qPCR (**C**) for measuring protein and mRNA expression, respectively. Dot graphs show expression of the indicated genes from the treated macrophages. Data represent mean ± SD (n = 4 or 6 per group).

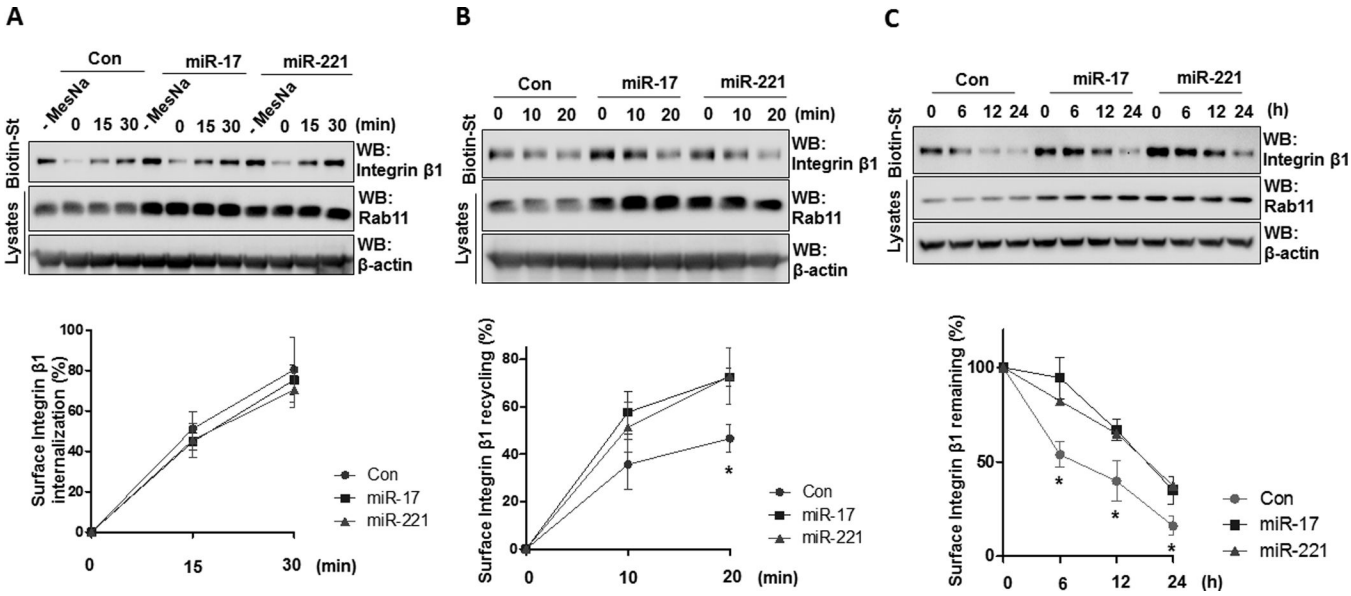

Figure 8. miR-17 and 221 promote endocytic recycling of integrin β1 in macrophages

A–C. THP1-differentiated macrophages were transfected with miR-17 or 221 mimics. Surface proteins of the macrophages were labeled with EZ-Link Sulfo-NHS-SS-Biotin, followed by surface integrin internalization (**A**), endocytic recycling (**B**), and degradation assay (**C**). Biotinylated proteins were precipitated with streptavindin, followed by Western blot analysis. Data represent mean ± SD (n = 3 per group).

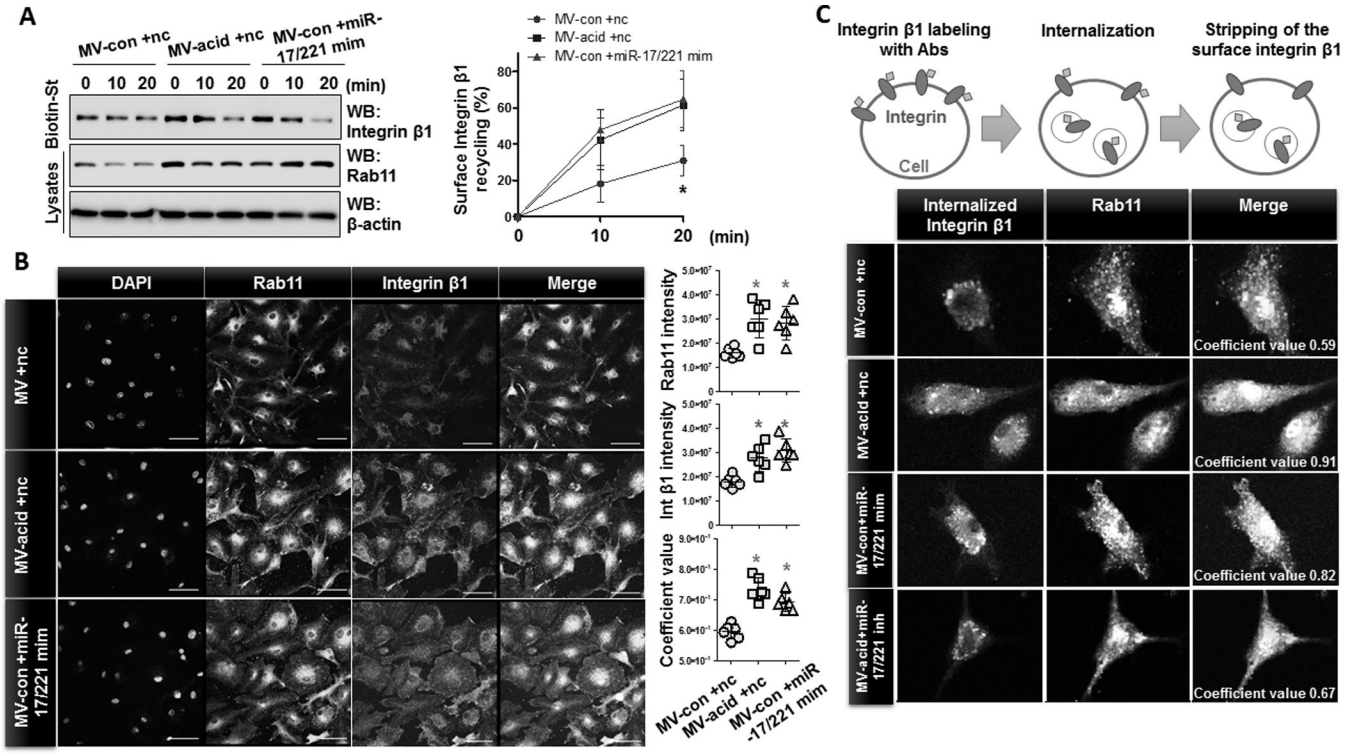

Figure 9. MV-containing miR-17/ 221 induce the trafficking of integrin β1 into recycling endosomes

A–B. MVs were isolated from control mice (MV-con) and mice after acid instillation (MV-acid). miR-17 and 221 mimics were directly transfected into MV-con (MV-con +miR-17/221 mim), as described in Materials and Methods. Non-specific RNA oligos were transfected into MVs as negative controls (MV-con +nc and MV-acid +nc). BMDMs were treated with the transfected MVs for 1day, followed by recycling assays (**A**) and double-immunostaining (**B**) using the indicated antibodies. Data represent mean ± SD (n = 3 or 6 per group). **C.** BMDMs were treated with the transfected MVs as described in (**A**), followed by labeling of surface integrin β1. Data are representative of three independent experiments. Scale bars = 50 μm.

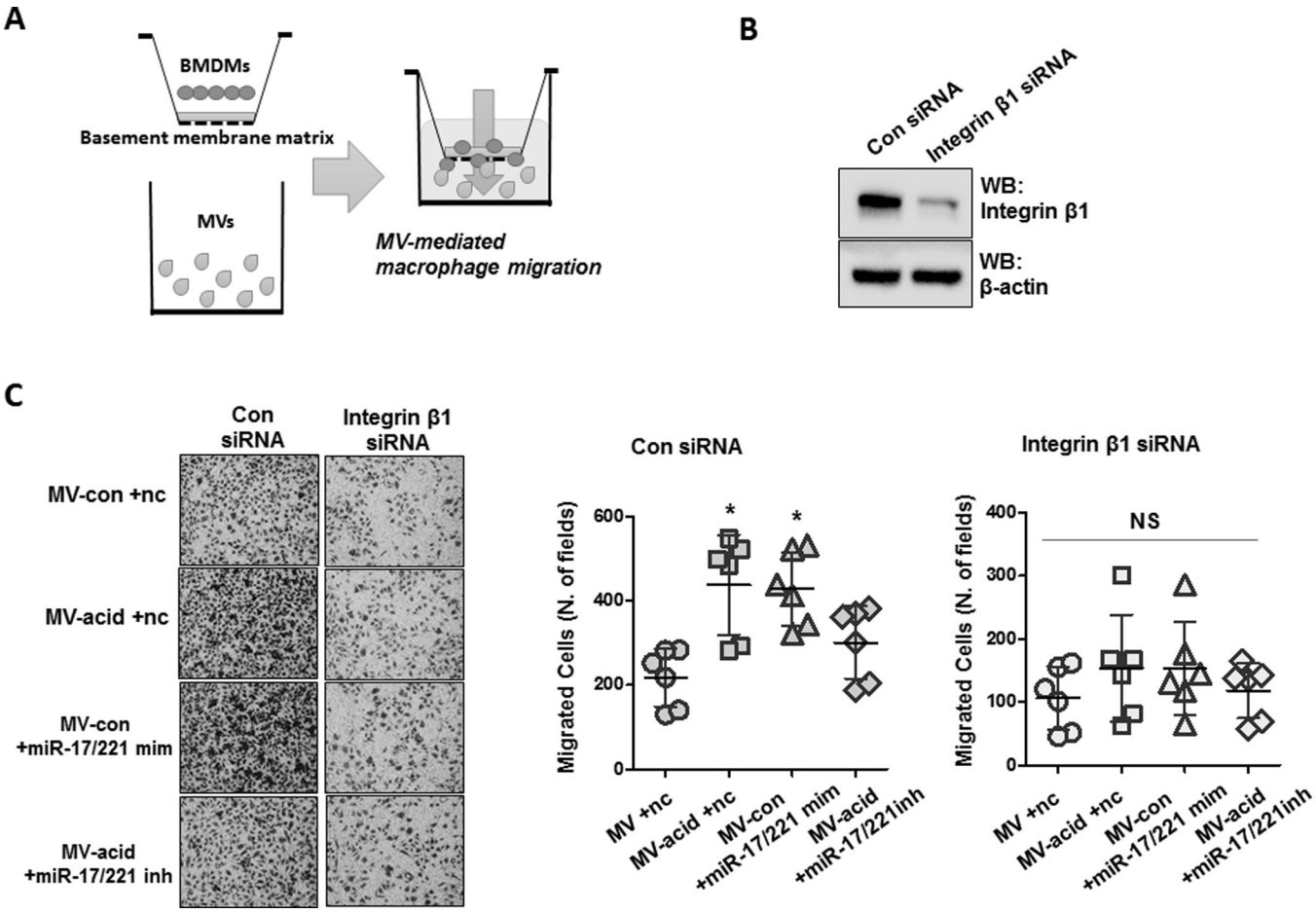

Figure 10. Integrin β1 is required for MV-miR-17 / 221-induced macrophage migration

A–C. Schematic illustration of the functional analysis of MV-containing miRNAs on macrophage migration (**A**). BMDMs were transfected with control siRNAs or integrin β1 siRNAs (50 nM) and expression levels of integrin β1 in the transfected BMDMs were assessed by Western blot (**B**). BALF-MVs were prepared as described in figure 3D, and transwell inserts were coated with basement membrane matrix. Migration assays of the transfected BMDMs were performed as described in Materials and Methods (**C**, left panel). Dot graph shows the migrated cell counts in each field (**C**, right panel). Data represent mean ± SD (n = 6 per group).

Table 1

Sequences of primers used in qPCR

Name	primer sequence for RT (5’ to 3’)	primer sequence for qPCR (5’ to 3’)
Universal primer		GGTGTCGTGGAGTCGGCAATTCAGTTGAG
miR-221	CTCAACTGGTGTCGTGGAGTCGGCAATTCAGTTGAGGAAACCCA	ACACTCCAGCTGGGAGCTACATTGTCTGCT
miR-320a	CTCAACTGGTGTCGTGGAGTCGGCAATTCAGTTGAGTCGCCCTC	ACACTCCAGCTGGGAAAAGCTGGGTTGAG
miR-92a	CTCAACTGGTGTCGTGGAGTCGGCAATTCAGTTGAGACAGGCCG	ACACTCCAGCTGGGTATTGCACTTGTCCC
miR-17	CTCAACTGGTGTCGTGGAGTCGGCAATTCAGTTGAGCTACCTGC	ACACTCCAGCTGGGCAAAGTGCTTACAGT
miR-185	CTCAACTGGTGTCGTGGAGTCGGCAATTCAGTTGAGTCAGGAAC	ACACTCCAGCTGGGTGGAGAGAAAGGCAGT
miR-21	CTCAACTGGTGTCGTGGAGTCGGCAATTCAGTTGAGTCAACATC	ACACTCCAGCTGGGTAGCTTATCAGACTGA
miR-20a	CTCAACTGGTGTCGTGGAGTCGGCAATTCAGTTGAGCTACCTGC	ACACTCCAGCTGGGTAAAGTGCTTATAGT
miR-93	CTCAACTGGTGTCGTGGAGTCGGCAATTCAGTTGAGCTACCTGC	ACACTCCAGCTGGGCAAAGTGCTGTTCGTG
miR-181a	CTCAACTGGTGTCGTGGAGTCGGCAATTCAGTTGAGACTCACCG	ACACTCCAGCTGGGAACATTCAACGCTGTC
let-7b	CTCAACTGGTGTCGTGGAGTCGGCAATTCAGTTGAGAACCACAC	ACACTCCAGCTGGGTGAGGTAGTAGGTTGT
Rab11		Forward: TGGGAAAACAATAAAGGCACAGA Reverse: ATGTGAGATGCTTAGCAATGTCA
Integrin β1		Forward: ATGCCAAATCTTGCGGAGAAT Reverse: TTTGCTGCGATTGGTGACATT
Rab4		Forward: GGAGCGGTTCAGGTCTGTG Reverse: AGTAAGCGCATTGTAGGTTTCTC
β-tubulin		Forward: CTGGGAGGTGATCGGGGAA Reverse: GCACATACTTCTTACCGTAGGCT
pre-mir-17		Forward: GTCAGAATAATGTCAAAGTGCTTAC Reverse: GTCAGCATAATGCTACAAGTGCCC
pre-mir-221		Forward: ATCCAGGTCTGGGGCATGAA Reverse: TTCCAGGTAGCCTGAAACCC
pre-mir-92a		Forward: CTTTCTACACAGGTTGGGATTTG Reverse: CCAAACTCAACAGGCCGGGA
pre-mir-320a		Forward: GCCTCGCCGCCCTCC Reverse: CCCACATCCTTTTTCGCCCT